Submitted to Acta Metallurgica

RECEIVED
LAWRENCE
RADIATION LABORATORY

APR 1 1974

LIBRARY AND
DOCUMENTS SECTION

LBL-2570
Preprint c.2

INTERSTITIAL ORDER AND EMBRITTLEMENT IN Ta-C ALLOYS

P. Rao and G. Thomas

February 1974

Prepared for the U. S. Atomic Energy Commission
under Contract W-7405-ENG-48

TWO-WEEK LOAN COPY

This is a Library Circulating Copy which may be borrowed for two weeks. For a personal retention copy, call Tech. Info. Division, Ext. 5545

LAWRENCE BERKELEY LABORATORY
UNIVERSITY OF CALIFORNIA

LBL-2570 c.2

DISCLAIMER

This document was prepared as an account of work sponsored by the United States Government. While this document is believed to contain correct information, neither the United States Government nor any agency thereof, nor the Regents of the University of California, nor any of their employees, makes any warranty, express or implied, or assumes any legal responsibility for the accuracy, completeness, or usefulness of any information, apparatus, product, or process disclosed, or represents that its use would not infringe privately owned rights. Reference herein to any specific commercial product, process, or service by its trade name, trademark, manufacturer, or otherwise, does not necessarily constitute or imply its endorsement, recommendation, or favoring by the United States Government or any agency thereof, or the Regents of the University of California. The views and opinions of authors expressed herein do not necessarily state or reflect those of the United States Government or any agency thereof or the Regents of the University of California.

INTERSTITIAL ORDER AND EMBRITTLEMENT IN Ta-C ALLOYS

P. Rao[1] and G. Thomas[2]

1) General Electric Company, Corporate Research and Development, Schenectady, New York 12301.

2) Department of Materials Science and Engineering, College of Engineering, University of California and Inorganic Materials Research Division, Lawrence Berkeley Laboratory, Berkeley, California 94720.

ABSTRACT

The effects of carbon on the structure and mechanical properties of tantalum at 77°K, 196°K and 300°K have been investigated. The alloys contained 0.76, 1.27, 1.53 and 2.05 at %C as determined by He-3 activation analysis.

Interstitial ordering was observed in all alloys with the formation and growth of aligned particles in <110> causing tweed contrast in electron micrographs. Analyses of electron diffraction patterns indicated that the fully developed single phase structure which is attained in Ta 1.53 and 2 at % C corresponds to a tetragonal or orthorhombic ordered lattice of composition $Ta_{64}C$ or $Ta_{32}C$. A model to explain these structures based on carbon fluctuations on specific {110} Ta planes is suggested. The alloys become completely brittle and cleave along {110} when the ordered structure is fully developed i.e. when the carbon content is 1.53 at % or more. It is suggested that this embrittlement results from the severe elastic strains which arise due to ordering such that the restrictions on the elastic compliances can no longer be maintained.

I. INTRODUCTION

In recent years, evidence has been obtained by transmission electron microscopy which suggests that small concentrations (≈1 at. %) of interstitials (carbon,[1] oxygen,[2,3,4] nitrogen,[5] and hydrogen[6]) in the Group VB body centered cubic metals lead to interstitial ordering. This is of particular interest since ordering has never been detected in substitutional solutions at concentrations of the order of one atomic percent. The elastic deformation associated with interstitial solutions is very much greater than that in substitutional solid solutions, and hence elastic strains play a much greater role in the ordering transformation in interstitial alloys. However, elastic strains appear to be generally important in refractory "solid solution" alloys because of anisotropy effects as has been pointed out by Van Torne and Thomas[7].

The crystal structures of different interstitial alloys have not yet received extensive attention, but the results indicate that the structures vary from system to system. Carbon-tantalum[1], vanadium-oxygen[4] give rise to ordered structures which have been interpreted from electron diffraction data in terms of a tetragonal lattice of ideal composition $M_{64}I$ (M represents solvent and I the interstitial). However, this composition is not observed in niobium-oxygen. The situation in tantalum-oxygen[8] is not yet clearly resolved. Beshers[9] has drawn attention to the fact that anisotropy effects determine the interstitial site occupancy in the solvent. He predicted that oxygen and nitrogen in Ta and Nb and nitrogen and carbon in vanadium would occupy tetrahedral interstices whereas carbon and nitrogen in α-iron, carbon in tantalum and oxygen in vanadium should prefer octahedral interstices.

These predictions so far appear to be in reasonable agreement with structural data derived from electron diffraction work. However, recent studies of the vanadium-nitrogen system[10] have reported the existence of the $V_{16}N$ structure wherein the nitrogen atoms occupy octahedral interstices, instead of the predicted tetrahedral sites[9]. Also, recent in situ studies of ordering in Ta-N utilizing high voltage electron microscopy [11] indicate that structures similar to those in Ta-C, but not V-N, are formed. Apart from the earliest reports[5] x-ray analysis has so far not been successfully utilized for structure analysis of order in interstitial alloys.

A well known, but relatively little understood, phenomenon in transition metals containing interstitial solutes is that of the ductile-brittle transition. This phenomenon of embrittlement depends upon solute content and testing temperature. Interstitial solutes such as hydrogen, carbon, nitrogen and oxygen are much more soluble in the Group VB metals (V, Nb, Ta) than in the Group VIB metals (Cr, Mo, W) and have a marked effect in producing embrittlement. Hydrogen is the most effective embrittling agent for V, Nb and Ta, while nitrogen, oxygen and carbon, in decreasing order, are less effective.

The purpose of this investigation is to follow in detail in Ta-C alloys the changes in microstructure and tensile mechanical properties accompanying the interstitial ordering transformation, utilizing transmission electron microscopy and diffraction. A field-ion microscopy investigation of Ta-C has been reported previously[12].

II. EXPERIMENTAL PROCEDURE

A. Specimen Preparation

High purity single crystals of tantalum were obtained from stock by electron beam zone refining. The single crystals were then rolled into strips 0.005 inch thick using a precision rolling mill, annealed at 2000°C for 2 hours in a dynamic vacuum of 10^{-7} mm Hg. All the specimens were treated similarly and allowed to cool in the furnace under vacuum so as to minimize impurity pickup and to obtain a uniform grain size.

Controlled amounts of carbon were vacuum deposited on both surfaces of the tantalum strips which were then annealed in the range 1000-2000°C (depending on composition) for 24 hours under high vacuum.

Heat treatments were done with reference to the existing phase diagram and from previous knowledge that Ta-1.56 at % C is ordered[1]. The existing phase diagram predicts virtually no solid solution range below about 2000°C for alloys containing less than about 1.5 at % carbon. Thus the final heat treatments were performed on the prepared alloys by annealing at 2000°C for 2 hours and furnace cooling. Uniform grain sizes ≈400μ were produced in each case. This treatment should produce ordering on cooling in all alloys because the kinetics for carbon diffusion are sufficiently rapid. However, aging treatments were also given to the Ta-0.76 and 1.53 at % carbon alloys in order to determine the effects of aging on its structure and mechanical properties. These aging treatments consisted of 6, 12, 36 and 72 hours annealing at 800°C under high vacuum followed by furnace cooling. Again 800°C was chosen as a temperature likely to be well below the solvus limit for this alloy, although it should be emphasized that the

critical temperatures for ordering are not known (and are not readily determined).

B. Analysis of Carbon Content Using Helium-3 Activation Analysis

A single, rapid and absolute method for detection of carbon and other elements over the concentration range of 1 ppb to 100% is helium-3 activation analysis[13]. Only a few milligrams of the total sample material are required. The key feature of this method is the use of He-3 ions accelerated to comparatively low kinetic energies so as to induce nuclear reactions which give radioactive products. These products, which decay mainly by emission of positrons or negatrons, can be detected by conventional nuclear techniques. In the case of carbon, the C^{12} (He-3,α)C^{11} reaction is used. The analysis was done by bombarding the specimens (placed after two 0.005 inch aluminum foils and one 0.005 inch gold foil to decrease the energy of the beam) with a 30 MeV He-3 beam from the Berkeley 88-inch cyclotron and measuring the α-decay rate as a function of time according to the above nuclear reactions. The carbon contents so obtained were 0.76 ± 0.0076, 1.27 ± 0.0127, 1.53 ± 0.0153 and 2.05 ± 0.0205 atomic percent respectively. The oxygen content was 0.02 atomic percent maximum.

C. Determination of Tensile Properties

Tensile specimens from strip tantalum, treated as above, were tested at three temperatures 300°K, 196°K and 77°K using the Instron universal testing machine at a strain rate of 3.33×10^{-4} sec^{-1}. The tensile specimens were 1/2 inch wide, had a one-inch gage length, and were 0.005 inch thick.

D. Electron Microscopy

Foils suitable for transmission electron microscopy were easily prepared by chemical polishing in a solution of 3:1 HNO_3:HF at or slightly below room temperature.

Observations were made using the Siemens IA electron microscope equipped with a double-tilting stage. Great care was taken to ensure that phase transformations were not induced during observation (see e.g. Ref. 2). Most of the foils obtained had either a <112> or <113> orientation. Since a [100] orientation is needed to uniquely characterize the morphology of the ordered phase, a 15° wedge had to be used in the double tilt holder of the Siemens electron microscope in order to obtain the [100] orientation.

Dark field images of superlattice reflections from ordered regions are necessary in characterizing the structure since coherency strains tend to obscure the morphological details in bright-field images or in dark-field images of fundamental reflections.

III. EXPERIMENTAL RESULTS AND INTERPRETATION

A. Determination of Tensile Properties

Figures 1a, 1b and 1c show a series of tensile stress-strain curves for specimens with varying carbon content, at three temperatures 300°K, 196°K and 77°K. The effect of increasing the interstitial content is to shift the curve in the plastic strain range to higher stress levels. The effect of decreasing temperature is similar in that at any one carbon composition, the specimens yield at higher stress levels with decreasing temperature.

Upper yield points were observed for all the alloys. The shear stress at lower yield τ_{LY} is a more reproducible measure of the strength of the specimen since τ_{LY} is not sensitive to specimen alignment in the tensile machine as τ_{UY} (τ refers to shear stress, which is taken as one-half the measured tensile stress σ)[7]. From Fig. 1 it can be seen that the plastic region of the stress-strain curve is nearly horizontal i.e., there is no appreciable increase in flow stress with strain to fracture. This is a common feature in polycrystalline bcc metals, particularly at room temperature[13].

It can been seen from Figures 1a, 1b and 1c that at any test temperature, the ductility (plastic regions of stress-strain curves) decreases with increasing carbon content, and all specimens containing 2.05 at % carbon are brittle. Figure 2 summarizes this ductile-brittle behavior and the results suggest that Ta-1.53 at. % carbon represents a critical composition for the onset of brittleness over the testing temperature range investigated.

When τ_{LY} is plotted vs. atomic percent carbon in tantalum, straight lines of positive slope result, as shown in Figure 3. The range of τ_{LY} observed is shown together with the average yield points for the three temperatures:

$$\text{AT } 300°\text{K}, \quad \tau_{LY} \left(\frac{kg}{mm^2}\right) = 6.0 + \{5.3 \times (\text{atomic percent carbon})\}$$

$$\text{AT } 196°\text{K}, \quad \tau_{LY} \left(\frac{kg}{mm^2}\right) = 12.2 + \{7.0 \times (\text{atomic percent carbon})\}$$

$$\text{AT } 77°\text{K}, \quad \tau_{LY} \left(\frac{kg}{mm^2}\right) = 26.4 + \{8.0 \times (\text{atomic percent carbon})\}$$

It can be seen that there is a very slight change in slope of the lines with temperature. Points marked B on the plot show the fracture stresses of those alloys exhibiting brittle failure (i.e., tantalum containing 2.05 at % carbon). The implications of this plot of τ_{LY} vs. at % carbon will be discussed later.

When the lower yield stress or fracture stress is plotted as a function of temperature, a series of curves are obtained one for each carbon composition as shown in Figure 4. There is an obvious increase in yield stress with decreasing temperature, and the lines curve upward with decreasing temperature. However, when specimens fracture before yielding (i.e., are brittle) there is practically a linear increase of fracture stress with decreasing temperature. It is observed that the ductility of tantalum containing 1.53 and 2.05 at % carbon varies only slightly with temperature as is shown in Figure 5 whereas the other alloys are all more ductile at the higher temperatures.

The yield strengths of the aged Ta-0.76 atomic percent carbon alloy is shown in a plot of yield strength vs. log aging time (Figure 6). No brittle behaviour was observed even after the longest aging time.

B. Electron Microscopy

In furnace cooled specimens, the microstructural changes with increasing carbon content are shown in Figure 7. The first resolvable structure is typical of the so called "tweed" contrast arising from strain contrast due to elastic deformation usually associated with large volume fractions of small coherent non cubic particles, or composition modulations (see e.g. Ref. 14 for review). Apart from apparent coarsening and obvious alignment in <110> this structure remains similar

in all alloys until the carbon content reaches 2.05 at % when single phase ordered grains containing antiphase domain boundaries are clearly resolved (Fig. 7e). The electron diffraction patterns corresponding to Figures 7a-d are shown in Figures 8a-d. As can be seen at Ta-1.5 at % C and Ta-2.05 at % C a superlattice of approximately [4 x 4]g<100> has developed. These results support the earlier results of Villagrana and Thomas[1] who concluded that the structure is consistent with a bc tetragonal structure of composition $Ta_{64}C$. However, other compositions such as $Ta_{32}C$ or $Ta_{16}C$ cannot be ruled out, because of multiplicity in the diffraction patterns. Figures 7 and 8 show that the fully ordered $Ta_{64}C$ structure is not developed by furnace cooling alloys until the carbon content attains 1.5%.

It can be seen in Figures 8b, c that the matrix reflections are streaked in <110>. This can be due to precipitation of thin sheets parallel to {110} and/or elastic strains in <100>, and is consistent with tweed contrast[15,16]. Figures 9 and 10 show examples of the development of this structure. Figure 10 indicates that the strain contrast in <110> is probably due to the alignment of small ordered particles in <110>. This is consistent with current models of tweed contrast[15]. However, images may also consist of net strain contrast when individual particles may not be resolved[14] especially if the strains are sufficiently large, and the strain fields overlap considerably. It should be noted that similar contrast effects have been observed in substitutional alloys showing short range order[17, 18].

It is known that elastic distortions due to coherent tetragonal particles produce streaking at reciprocal lattice points. Tyapkin[19]

has shown that coherency induces pure shear on $\{1\bar{1}0\}$ planes in <110> directions resulting in the extension of the diffracted intensity along the normal to the shear planes. The magnitude of the shear strain depends on the value of the anisotropy factor, A, defined as

$$A = \frac{G_{100}}{G_{110}} = \frac{2C_{44}}{(C_{11}-C_{12})}$$

When the cubic crystal is isotropic A = 1, while when A > 1, then G_{110} becomes a minimum. Since for Ta A = 1.58, and given the condition of tetragonality associated with ordering, there will be relatively low resistance to shear on {110} $<1\bar{1}0>$.

The results of the isothermal aging experiments are consistent with the development of periodic ordered arrays or particles. For example Figure 11 shows that after 72 hours aging at 800°C the 0.76 at % C alloy is similar in structure to that of the furnace cooled 1.26 at % C alloy. By comparison of Figures 11f, 6 and 4, it is also apparent that the yield stress and elongation values are also similar. That is the mechanical properties do not depend on carbon content alone, but on the degree of order or, from an alternative viewpoint, upon the volume fraction of the ordered phase present.

From these observations, it is concluded that in Ta-C the development of the long-range ordered superlattice proceeds by the formation, growth and coalescence of small ordered particles (Figures 9, 10). A mechanism for this process is proposed in the following, in which alternative compositions to $Ta_{64}C$ can be accounted for.

IV. DISCUSSION

A. Structure of the Ordered Phase

From previous studies[1], the superlattice in Ta-1 to 2 at. % C has been given the formula $Ta_{64}C$ and it was proposed that the unit cell is body-centered tetragonal. The fact that the unit cell of the ordered phase has orthogonal axes but is non-cubic, is beyond dispute (e.g. the observed diffraction patterns, the nature of the fringes at APBs and the tweed strain contrast). However, it should be emphasized that because of the multiplicity of orientations which contribute to the diffraction patterns, the complexities due to double diffraction, and the difficulties of sorting out the patterns by dark field analysis when the ordered particles cannot be individually resolved, do not permit unique establishment of the Bravais lattice at the present time. In fact, the diffraction patterns vary with carbon content,e.g. Figure 8 and examination of orientations such as <112> and <113> suggest that structures exist which may be base-centered orthorhombic (bco), but in which the a and b axes have only slightly different lengths. The composition is $Ta_{64}C$ if the unit cell is based on 4 x 4 x 4 tantalum cells or $Ta_{32}C$ if it is 4 x 4 x 2 or $Ta_{16}C$ if it is 4 x 4 x 1. More than one composition is of course possible, but until individual particles of the same orientation can be identified for structure analysis it is not possible to uniquely identify the ordered phase[5] by selected area diffraction {the smallest selected area possible at 100 kV is ≈2μ diameter and this is very large compared to the particle or domain size (see e.g. Figure 7)}. The use of lattice imaging in a high resolution electron microscope may help to untangle these complications.

B. Model for Development of the Ordered Phase

In spite of the difficulties outlined above, it is possible to arrive at a model for the development of the ordered phase which can account for tetragonal and orthorhombic structures (Figure 12). It is postulated that only four of the six possible {110} planes in bcc tantalum be occupied by carbon atoms exclusively. That this is reasonable follows by consideration of the nature of the octahedral sites. For example, consider that the carbon atoms in the ordered phase occupy specifically the $\frac{1}{2}00$ octahedral sites (that is, the c-axis of the unit cell is the [001] direction), then the planes containing only carbon atoms are the (110), $(1\bar{1}0)$ {both perpendicular to the (001) plane} and (101), $(10\bar{1})$ {both perpendicular to (010) planes}. These are the only planes containing carbon atoms exclusively, which can give rise to carbon concentration fluctuations in the ordered structure. Other combinations of {110} fluctuations are possible for the $0\frac{1}{2}0$ or $00\frac{1}{2}$ octahedral sites. These fluctuations are consistent with the observed contrast in the electron micrographs.

Figure 12 shows {001} projections which illustrate the possibilities that arise by such fluctuations. Only three alternatives occur, two with common carbon contents and two with common crystal structures. The (001) projection is common to all three cases and consequently is only shown once. Likewise, the (100) projection is the same for $Ta_{64}C$ (bco) and $Ta_{32}C$ (bco).

The interplanar spacing between these carbon containing {110} planes determines the composition of the ordered phase formed. In all cases, only two of the four {110} carbon containing planes are observed to have

a constant interplanar spacing such that $d_{110_C} = 4d_{110_{Ta}}$. These are the (110) and $(1\bar{1}0)$ planes {perpendicular to (001)}. However, the interplanar spacings between the (101) and $(10\bar{1})$ carbon containing planes {perpendicular to (010)} are observed to vary such that $d_{101_C} = 2d_{101_{Ta}}$. When $d_{101_C} = 2d_{101_{Ta}}$, either a $Ta_{64}C$ or $Ta_{32}C$ structure can be obtained by varying the carbon atom density on these planes, keeping the interplanar spacing constant (Figure 12).

In an interstitial alloy, the spacing between a carbon containing (110) plane and a neighboring Ta containing (110) plane is not the same as between two neighboring Ta containing (110) planes. The spacing in the former case is equal to 1/2 of that in the latter case.

Now assuming that a periodic fluctuation of carbon atoms in tantalum occurs, then the ordered structure can <u>only</u> be obtained when there are simultaneous carbon fluctuations on four of the six possible {110} type planes in a given region of the bcc tantalum. However, in the early stages of ordering, all four sets of fluctuation may not exist, and therefore, the diffraction pattern may not be fully developed. For example, every fluctuation with $d_{110_C} = 4d_{110_{Ta}}$ will give rise to a superlattice spot at $1/4g_{110_{Ta}}$. This is exactly what is observed during the early stages of the transformation (for example, Figure 8c). There is a superlattice spot at $1/4g_{110_{Ta}}$ around every matrix Ta spot, each set of spots in any one <110> direction being due to a set of fluctuations in that direction.

As the carbon concentration increases, the number of sets of {110} planes on which fluctuations can occur increases, so that the volume

fraction of ordered particles is expected to increase, and/or the carbon composition within a particle will increase. As in the spinodal, such a transformation may not require a nucleation stage. The diffusion process sets up regions of ideal wavelength. Once this ideal is obtained, an "ordered particle" with coherent interfaces is formed. The size of the ordered regions depends on the number of wavelengths involved in that set of fluctuations. The alignment of ordered regions or particles along {110} surely is a consequence of minimizing the strain energy. The degree of order may also vary not only from particle to particle, but also within each particle. Because of the complicated contrast in the images, the volume fraction of the ordered phase cannot be determined, but it is possible to conclude that the volume fraction is high (from images) and that the degree of order is probably varying (from diffraction patterns). Once the ordered regions are formed, they align themselves along <110> and grow into the disordered matrix till they impinge along common [100] directions (see Figure 10). It must be noted that although the domains impinge along [100] directions, they are probably bounded by (110) prism planes (as observed in the Nb-O system by Van Torne and Thomas[2]). The [100] impingement probably arises because four of the six possible (110) planes in a crystal cut any (001) surface along <100> directions. Further growth involves the formation of large cuboidal shaped particles bounded by (110) planes, aligned along <110>. The final stage involves the growth of crystals with one type of c-axis in preference to any other, to give rise to large non-impinging ordered domains.

C. Correlation of Mechanical Properties and Microstructure

Fractographic studies of the broken tensile specimens using scanning electron microscopy showed that the predominant mode of ductile failure was transgranular, but this changed from cleavage to microvoid coalescence and finally integranular fracture in the 2 at % C alloy[20]. The cleavage in brittle alloys was found to occur on {110}. There was no evidence for a carbide phase at the boundaries themselves. These results together with the observed increase in yield stress with carbon content (Figure 3) show that the matrix strength approaches that of the cleavage strength at 1.53 at. % C, depending on temperature.

The minimum cleavage shear stress will occur when the elastic shear strain energy is maximized in some region and direction in the crystal. One would expect the maximum shear strain energy to be attained in regions and directions which possess the largest internal strain energy. The maximum shear strain energy will be attained in regions which lie parallel to the cleavage plane. In tantalum, the cleavage plane is {110} as opposed to {100} in tungsten. Therefore, the maximum shear strain energy, on introduction of a critical concentration of interstitials should be attained on {110} planes.

When the alloys are brittle and cleave, the values of the elastic compliances are such that the restriction imposed on the compliances by a positive strain energy of a crystal are only marginally fulfilled. These restrictions are[7]:

(a) $S_{44} > 0$

(b) $S_{11} > S_{12}$

(c) $S_{11} + 2S_{12} > 0$

Substitution of the values of pure tantalum, $S_{11} = 6.78 \times 10^{-13}$ cm^2/dyne, $S_{12} = -2.47 \times 10^{-13} cm^2$/dyne and $S_{44} + 11.98 \times 10^{-13} cm^2$/dyne, shows that an increase in S_{12} of $0.92 \times 10^{-13} cm^2$/dyne is sufficient to violate the restriction $S_{11} + 2S_{12} > 0$. Therefore, it is conceivable that a point is reached in carbon composition where the restrictions on the compliances, which are the same as on the stiffnesses, are not satisfied. The crystal then becomes energetically unstable and it fails along a crystallographic set of planes which release a maximum amount of strain energy.

In the present work, it is observed that carbon causes a linear increase in yield strength and a decrease in ductility up to 1.56 at %. At this point, there is a sudden catastrophic loss in ductility. The linear dependence of yield stress on carbon composition reflects its dependence on the degree of order and on the volume fraction of the ordered phase. The onset of brittleness appears to coincide with the development of large scale ordered domains. If the above considerations regarding the elastic compliances are correct, the results suggest that the development of fully ordered domains corresponds to a critical carbon level such that the strain energy is so large that the restrictions on the compliances are no longer satisfied, and the crystals cleave. The maximum strain energy is reached on the {110} planes, which are also the observed cleavage planes.

V. SUMMARY

Carbon in tantalum produces interstitial ordering with the development of ordered phase(s) of composition $Ta_{64}C$ or $Ta_{32}C$, having tetragonal or orthorhombic lattices. Octahedral site occupancy predicted by Beshers[9] for carbon in tantalum is confirmed on the basis of the inequality

of the [100] and [001] dimensions as determined from electron diffraction data. Transmission electron microscopy indicates that the ordering transformation begins by fine scale fluctuations in carbon composition associated with the {110} planes. The fully ordered structure is realized locally when regions of wavelength such that $\lambda_C = 4d_{110_{Ta}}$, $2d_{101_{Ta}}$ or $d_{101_{Ta}}$ are obtained. The alloy can be considered then to contain small "ordered particles". These small ordered regions align themselves along <110> and grow till impingement. The final stage of the ordering transformation occurs with the formation of long range highly ordered regions separated by coherent domain boundaries and is observed in the Ta-1.53 and Ta-2.05 at % C alloys. At this stage the alloys become totally brittle. It is suggested that this embrittlement is caused by severe elastic strains resulting from carbon ordering such that the restrictions on the elastic compliances cannot be maintained.

ACKNOWLEDGMENTS

We wish to acknowledge financial support from the United States Atomic Energy Commission through the Inorganic Materials Research Division of the Lawrence Berkeley Laboratory for this research. This work was done in partial fulfillment of the Ph.D. degree at Berkeley by one of the authors (PR).

REFERENCES

1. R. E. Villagrana and G. Thomas, Phys. Stat. Sol. 9, 499 (1965).
2. L. I. Van Torne and G. Thomas, Acta Met. 12, 601 (1964).
3. J. Van Landuyt, R. Gevers and S. Amelinckx, Phys. Stat. Sol 13, 467, (1966).
4. J. W. Edington and R. E. Smallman, Acta Met. 13, 155 (1965).
5. D. P. Seraphim, N. R. Stemple and D. T. Novick, J. Appl. Phys. 33, 136 (1962).
6. D. Hull and D. C. Wynne, Proceedings of the Third European Regional Conference on Electron Microscopy, Prague, 1964; Czeck. Acad. Sci., Prague, 1964 (p. 239).
7. L. I. Van Torne and G. Thomas, Acta Met. 14, 621 (1966).
8. R. H. Geiss and K. R. Lawless, Scripta Met., 2, 254 (1970).
9. D. N. Beshers, J. Appl. Phys. 36, 290 (1964).
10. D. Potter and C. Altstetter, Acta Met. 19, 881 (1971), also ibid 20, 313 (1972).
11. P. R. Swann, G. Thomas and N. J. Tighe, J. Microscopy, 97, 249 (1973).
12. P. Rao, Proceedings of the Twenty Eighth Annual Meeting of the Electron Microscopy Society of America, Claitor's Publishing Division, Baton Rouge, La., 1970 (p. 532).
13. S. S. Markowitz and J. D. Mahony, Anal. Chem. 34, 329 (1962).
14. G. Thomas, in Modern Diffraction and Imaging Techniques in Materials Science, Eds. S. Amelinckx et al., American Elsevier Publishing Co., New York p. 131, (1970). (New edition in press 1974)
15. P. J. Fillingham, H. J. Leamy and L. E. Tanner, Electron Microscopy and Structure of Materials, Ed. G. Thomas, R. M. Fisher and R. M. Fulrath, University of California Press 1972, p. 163.

16. L. E. Tanner, Phil. Mag. 14, 111 (1966).

17. P. R. Okamoto and G. Thomas, Acta Met. 19, 825, (1971); S. K. Das, P. R. Okamoto, P.M.J. Fisher and G. Thomas, ibid., 21, 913 (1973).

18. H. Warlimont and G. Thomas, Met. Sci. J. 4, 17 (1970).

19. Y. D. Tyapkin, Sor. Phys. Dok. 9, 95 (1964).

20.. P. Rao, Ph.D. Thesis, University of California, Berkeley (1969), UCRL-19113.

FIGURE CAPTIONS

FIG. 1. Stress-strain curves of tantalum containing up to 2.05 at %C t tested at 300°K (a), 196°K (b), and 77°K (c).

FIG. 2. Summary of ductile-brittle behavior of tantalum-carbon alloys containing up to 2.05 at %C in a plot of test temperature (°K) vs. atomic percent carbon in tantalum.

FIG. 3. Plot of shear stress at lower yield, τ_{LY}, vs. atomic percent carbon in tantalum. The grain size is ≈400μ in all cases.

FIG. 4. Plot of stress (kg/mm^2) at lower yield or fracture vs. test temperature (°K).

FIG. 5. Plot of total elongation (%) vs. test temperature (°K).

FIG. 6. Plot of yield stress (kg/mm^2) vs. log aging time (hours) for a Ta-0.76 at %C alloy aged at 800°C for 6, 12, 36 and 72 hours. (Tested at 300°K).

FIG. 7. Bright field electron micrographs of various stages of the interstitial ordering transformation:

(a) Pure tantalum

(b) Ta-0.76 at %C showing contrast due to fine fluctuations in carbon composition.

(c) Ta-1.27 at %C showing the formation of "ordered" particles which align themselves along the <110> directions.

(d) Ta-1.53 at %C showing growth along <110> till impingement.

(e) Ta-2.05 at %C showing the formation of highly ordered regions separated by coherent antiphase domain boundaries.

FIG. 8. Electron diffraction patterns obtained from each of the above stages of the ordering transformation. Figure 8a corresponds to

the diffraction pattern obtained from Figure 7a etc.

FIG. 9. Bright field (a) and dark field (b) images obtained from Ta-0.76 at % carbon showing a rather diffuse tweed contrast. Matrix spots in diffraction patterns are streaked in <110> normal to the {110} striations in contrast.

FIG. 10. Bright field (a) and dark field (b,c and d) images from Ta-1.53 at %C showing the formation of impinging small-to-medium sized domains. Figures 10a and 10b are obtained using matrix reflections while Figures 10c and 10d are obtained using superlattice reflections.

FIG. 11. Bright field (a.c,d and f) and dark field (b and e) images of Ta-0.76 at %C aged at 800°C for 6 hours (a,b), 12 hours (c), 36 hours (d,e) and 72 hours (f).

FIG. 12. {001} projections showing structures generated by fluctuations in carbon composition resulting from exclusive occupancy of carbon atoms (large circles) on the specific {110} planes indicated below each projection. Filled small circles shows Ta atoms. Carbon atoms not in the plane of projection are shown as dashed circles (see text). The various possibilities generate either $Ta_{64}C$ (bct or bco) or $Ta_{32}C$ (bco) structures.

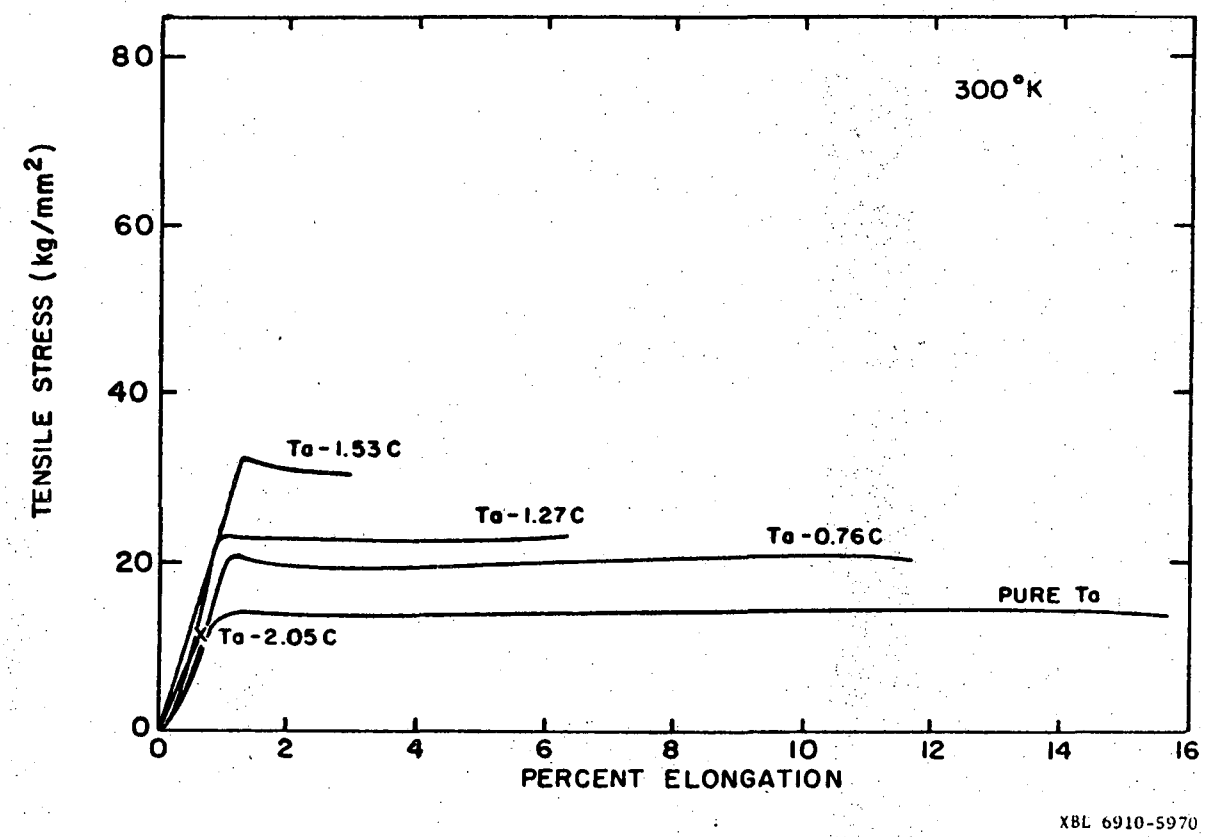
300°K
TENSILE STRESS (kg/mm²)
PERCENT ELONGATION
Ta-1.53C
Ta-1.27C
Ta-0.76C
PURE Ta
Ta-2.05C
0
20
40
60
80
0
2
4
6
8
10
12
14
16
XBL 6910-5970

Fig. 1a

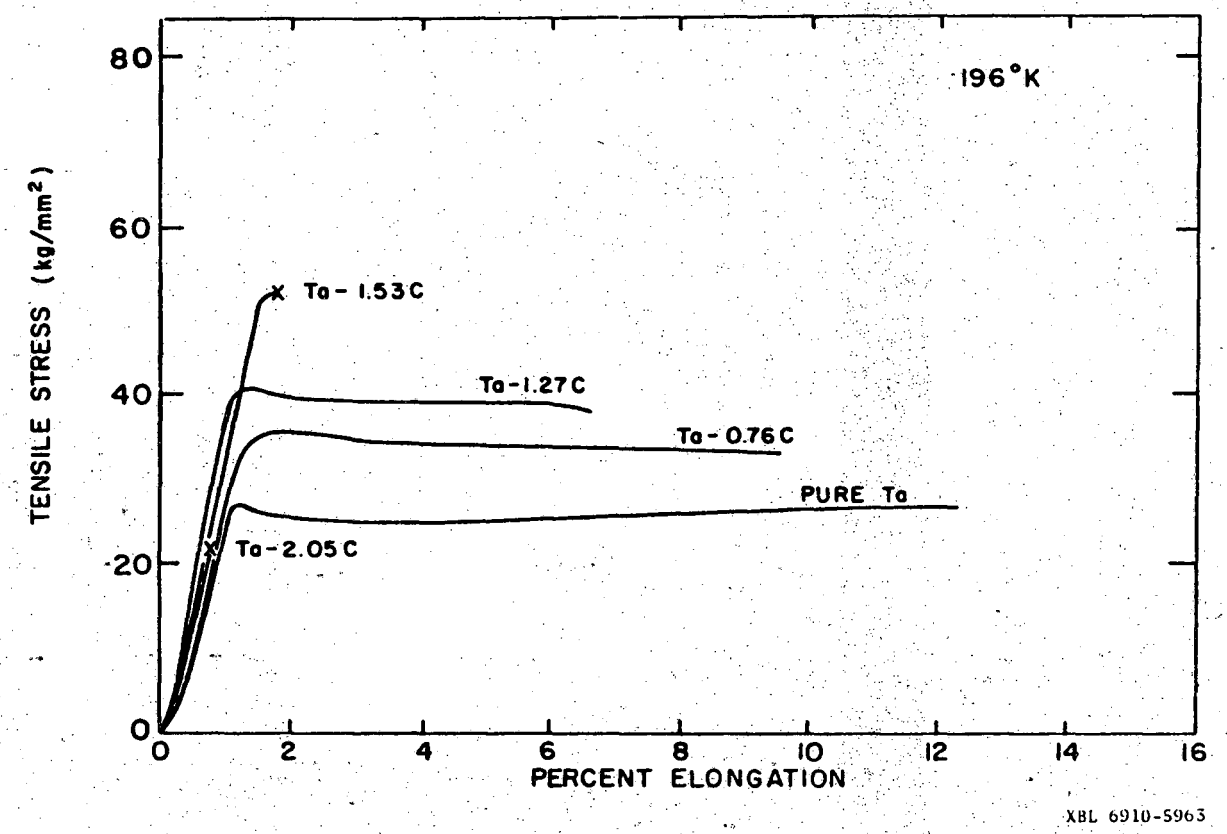
196°K
TENSILE STRESS (kg/mm²)
PERCENT ELONGATION
Ta - 1.53C
Ta-1.27C
Ta-0.76C
PURE Ta
Ta-2.05C
0
20
40
60
80
0
2
4
6
8
10
12
14
16
XBL 6910-5963

Fig. 1b

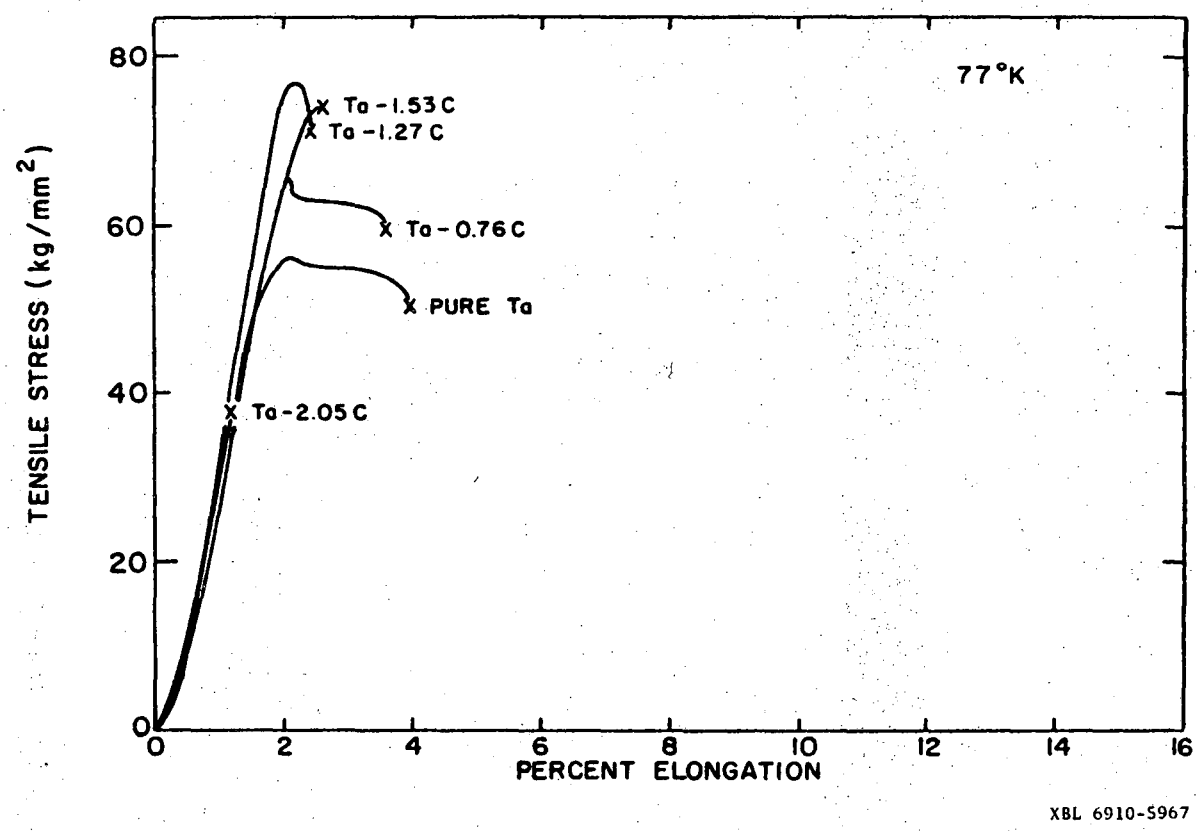
77°K
Ta-1.53 C
Ta-1.27 C
Ta-0.76 C
PURE Ta
Ta-2.05 C
TENSILE STRESS (kg/mm²)
PERCENT ELONGATION
0
20
40
60
80
0
2
4
6
8
10
12
14
16
XBL 6910-5967

Fig. 1c

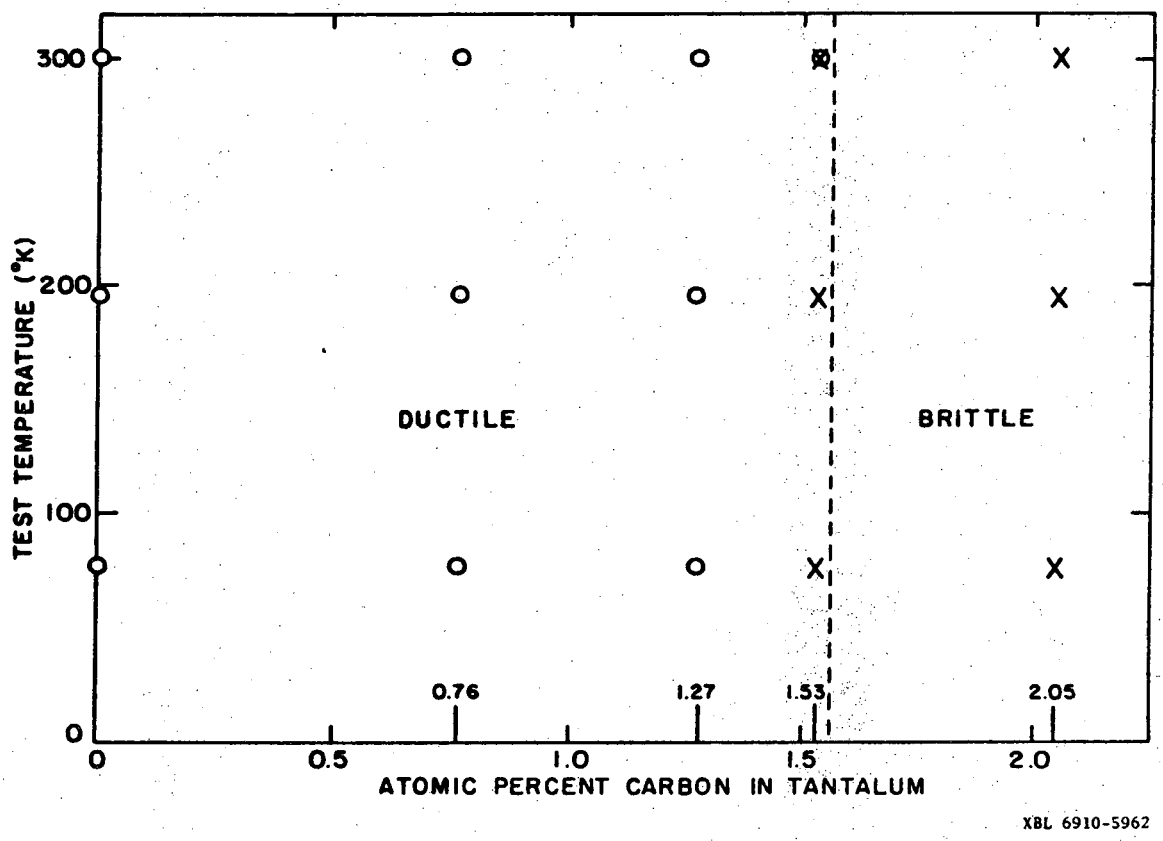
300
200
100
0
TEST TEMPERATURE (°K)
DUCTILE
BRITTLE
0.76
1.27
1.53
2.05
0
0.5
1.0
1.5
2.0
ATOMIC PERCENT CARBON IN TANTALUM
XBL 6910-5962

Fig. 2

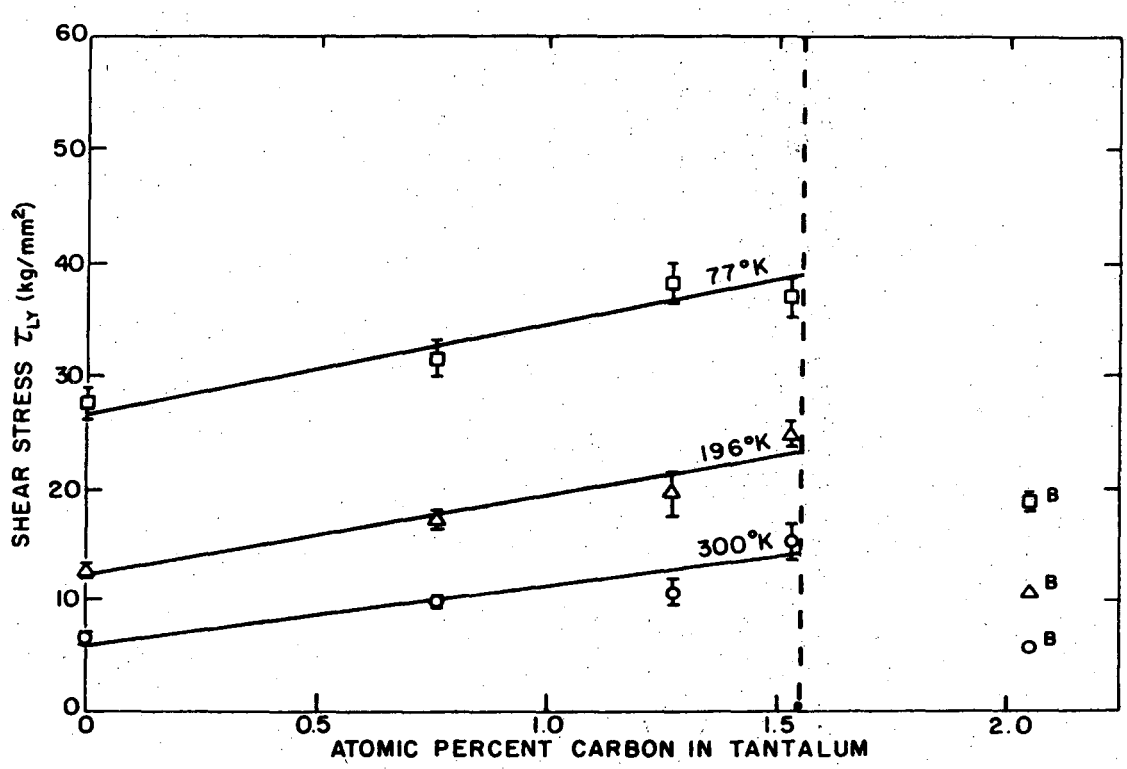

XBL 6910-5961-A

Fig. 3

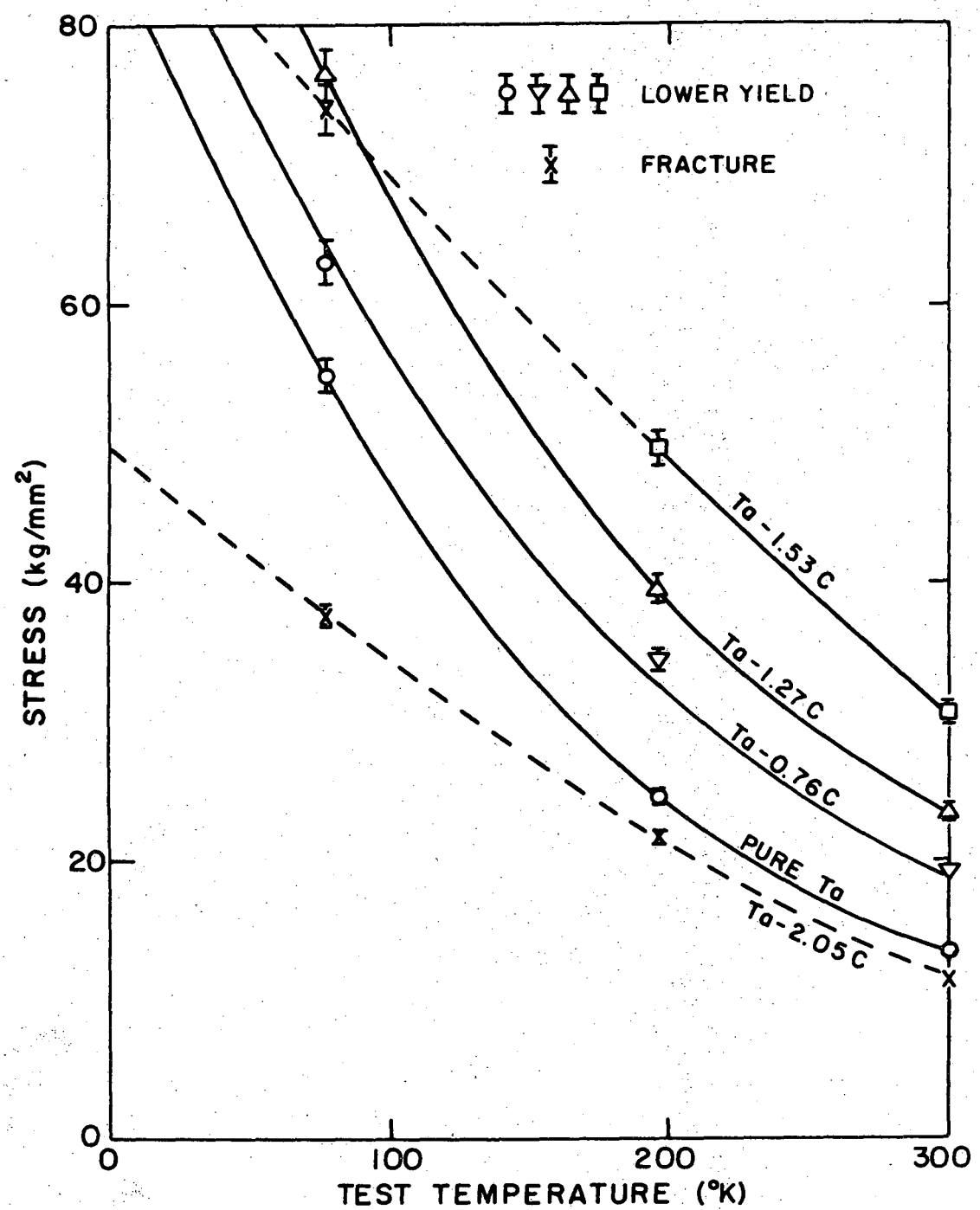

XBL 6910-5959

Fig. 4

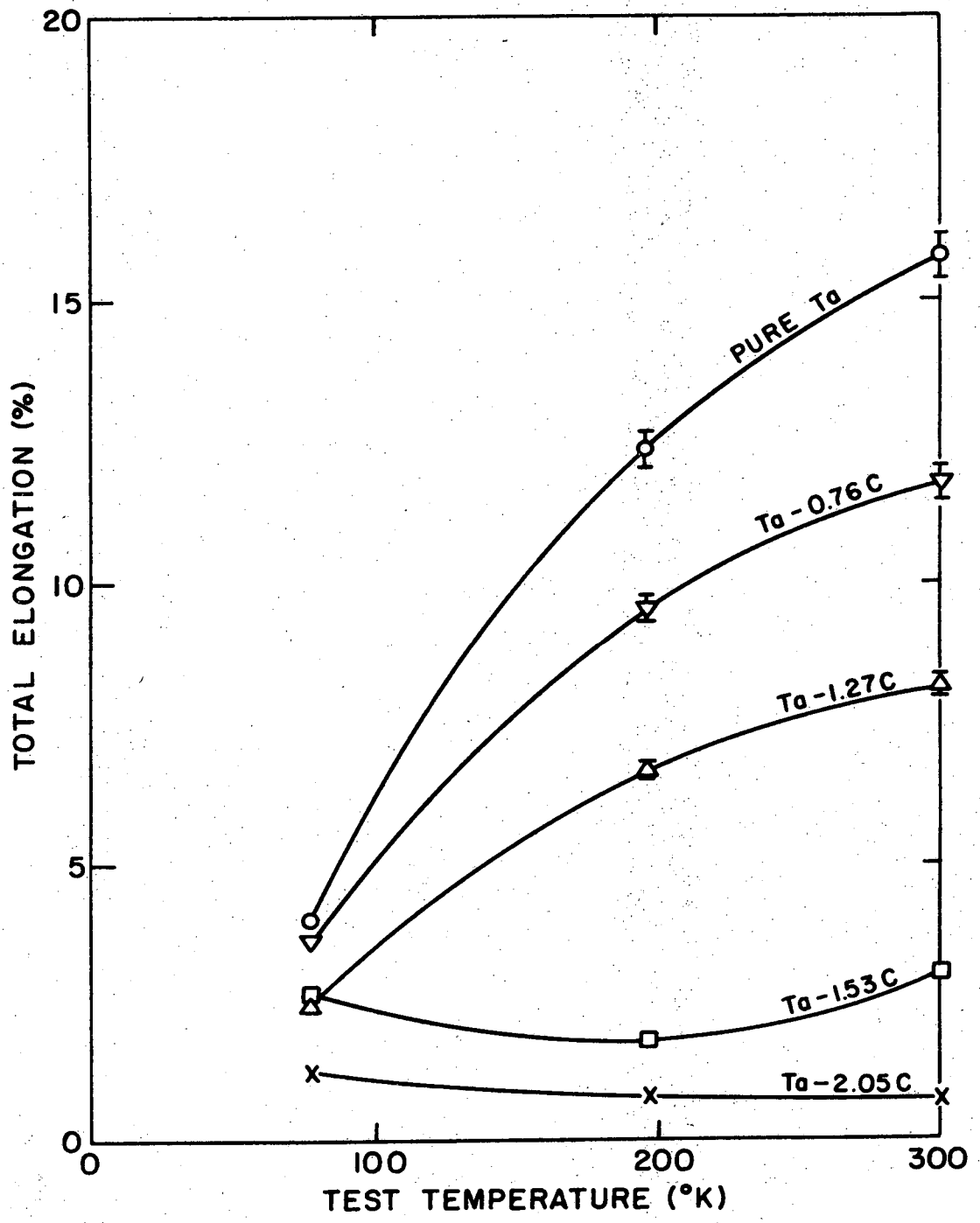

XBL 6910-5957

Fig. 5

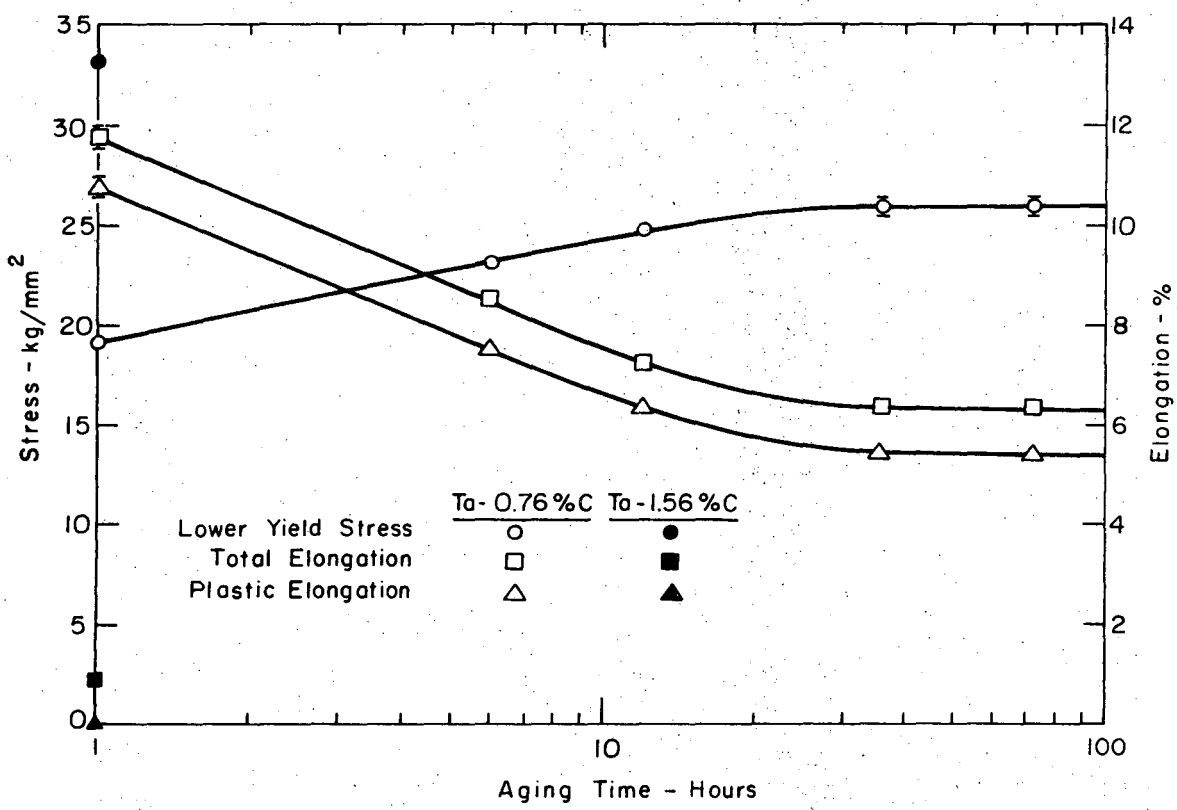

XBL729-6976

Fig. 6

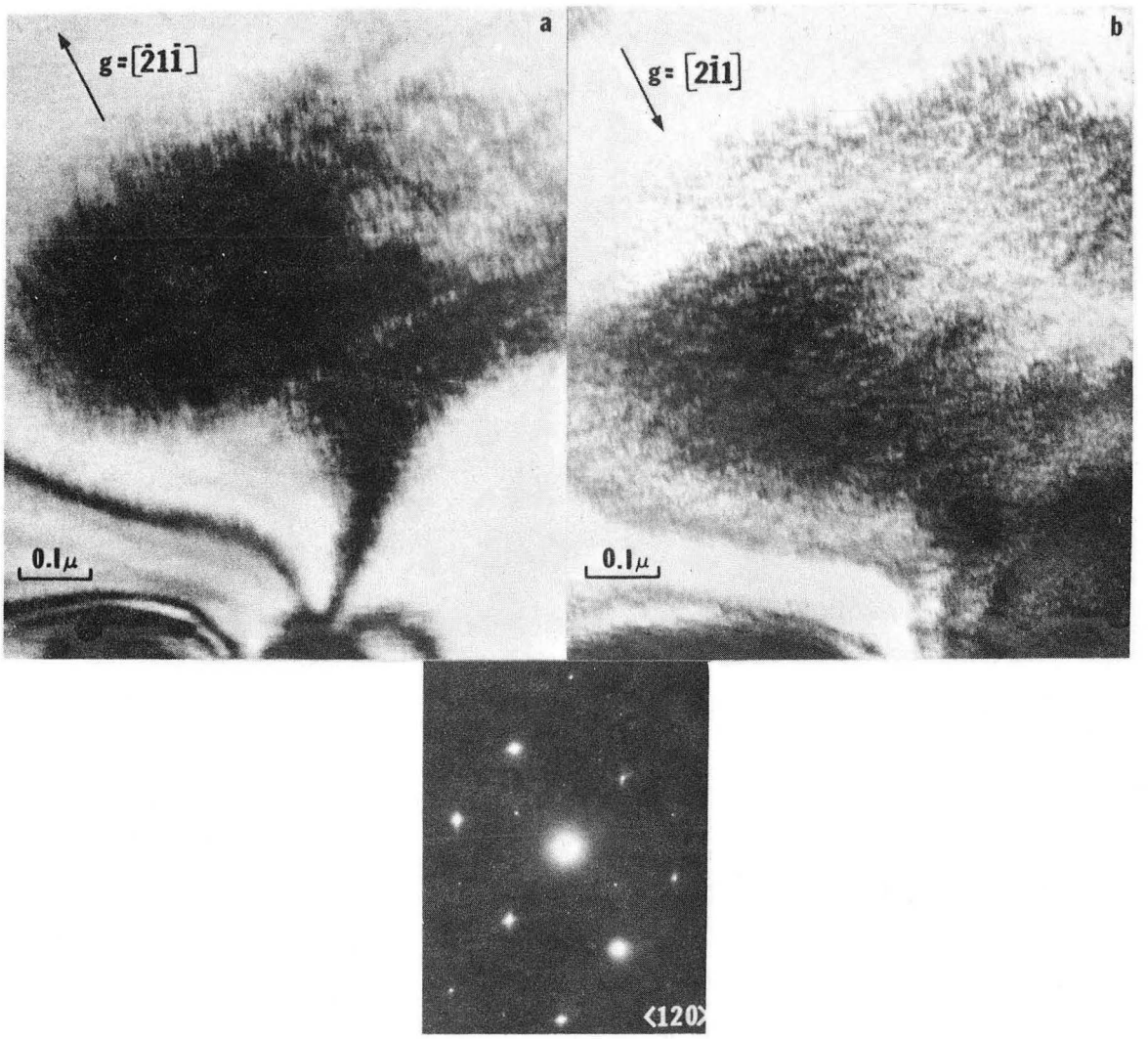

XBB 6911-7117

Fig. 9

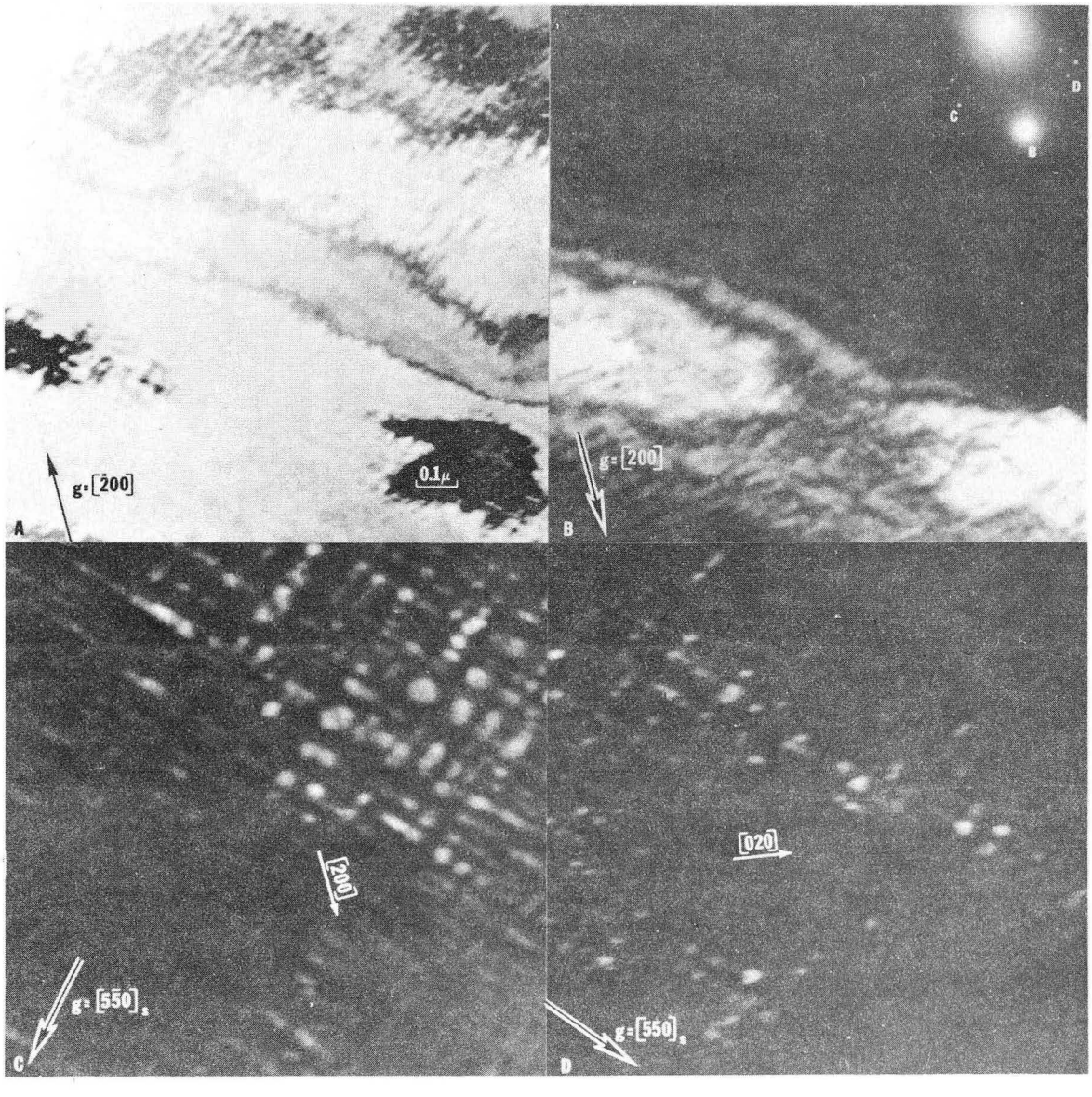

XBB 6911-7116

Fig. 10

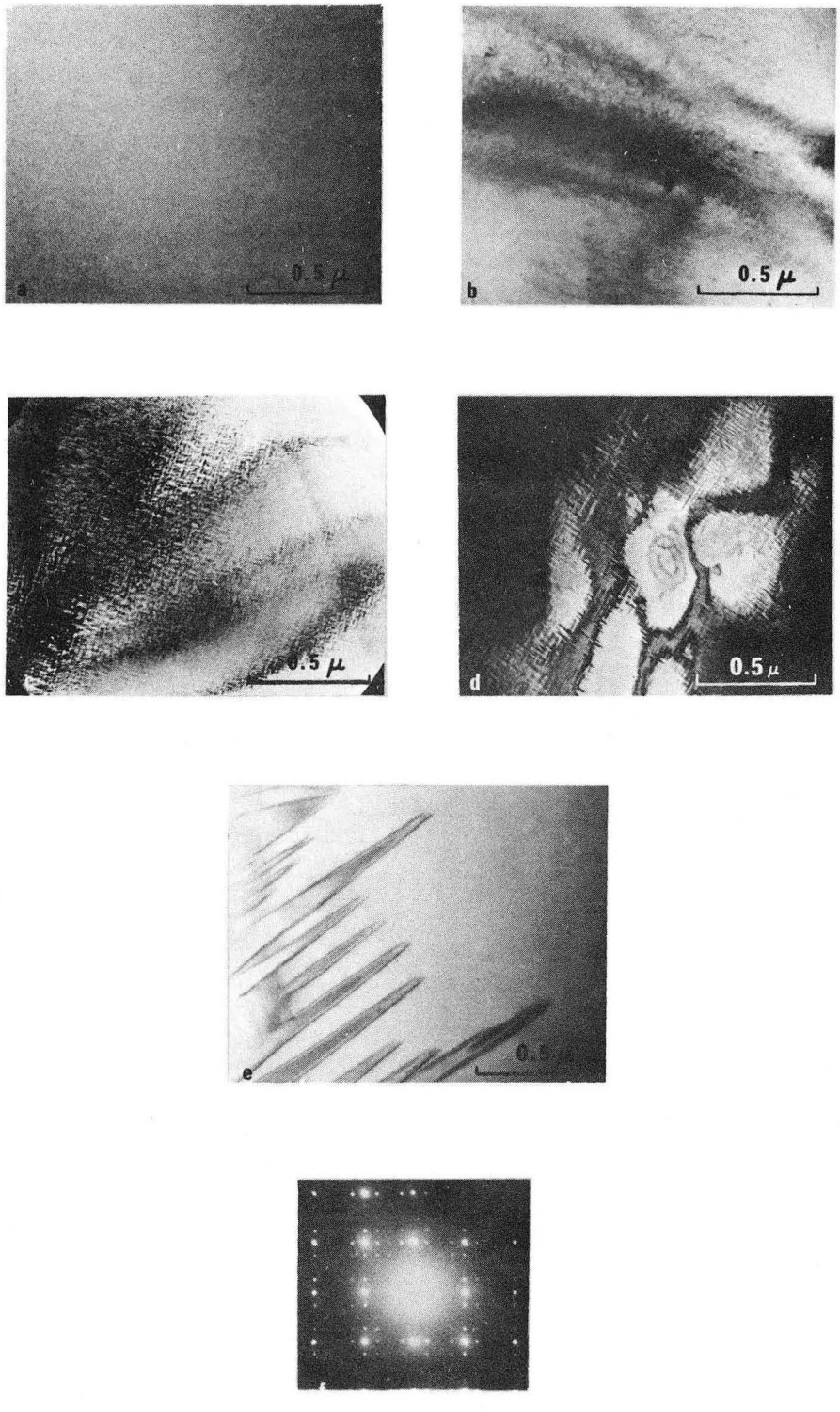

XBB 6911-7115

Fig. 7

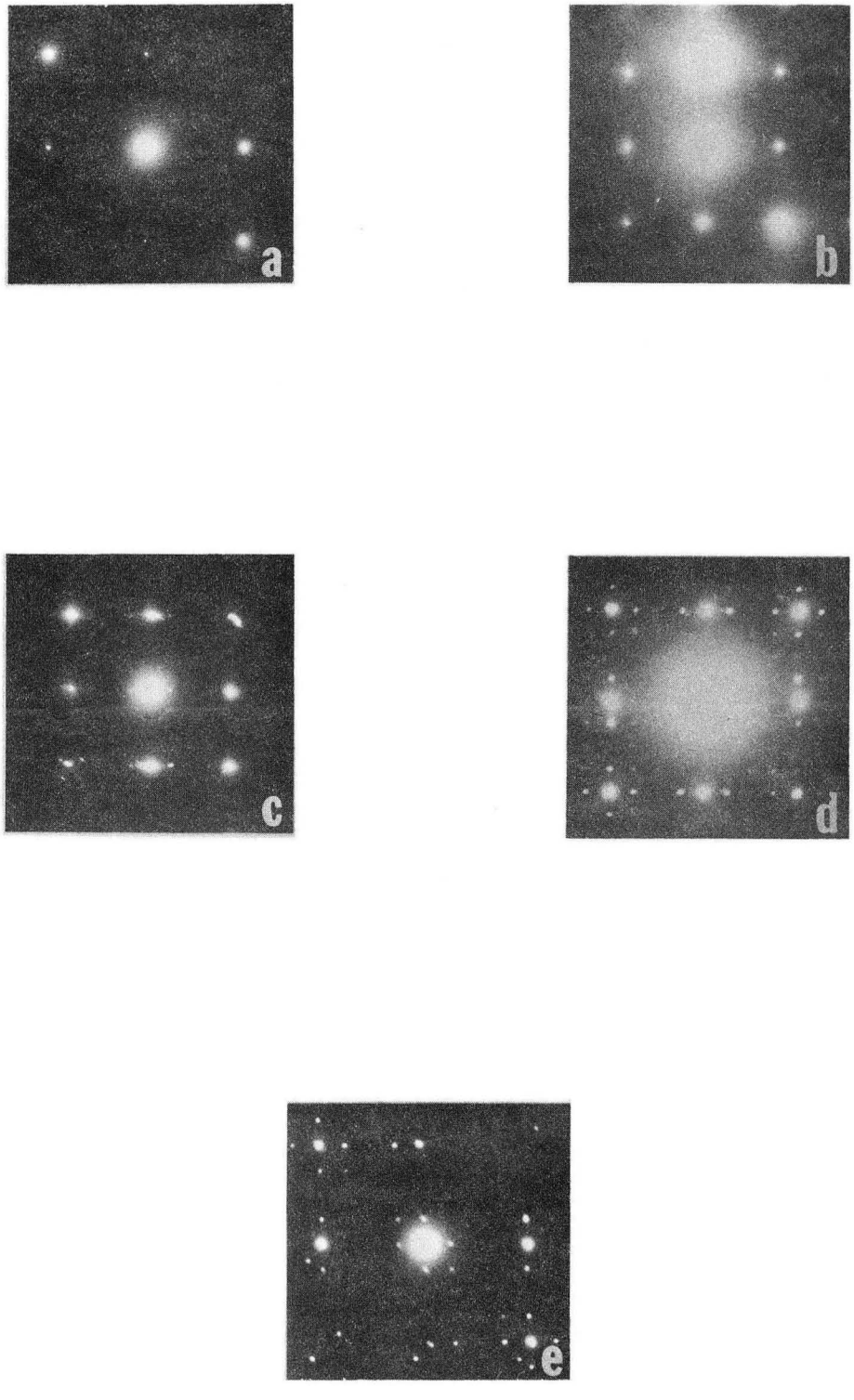

XBB 6911-6114

Fig. 8

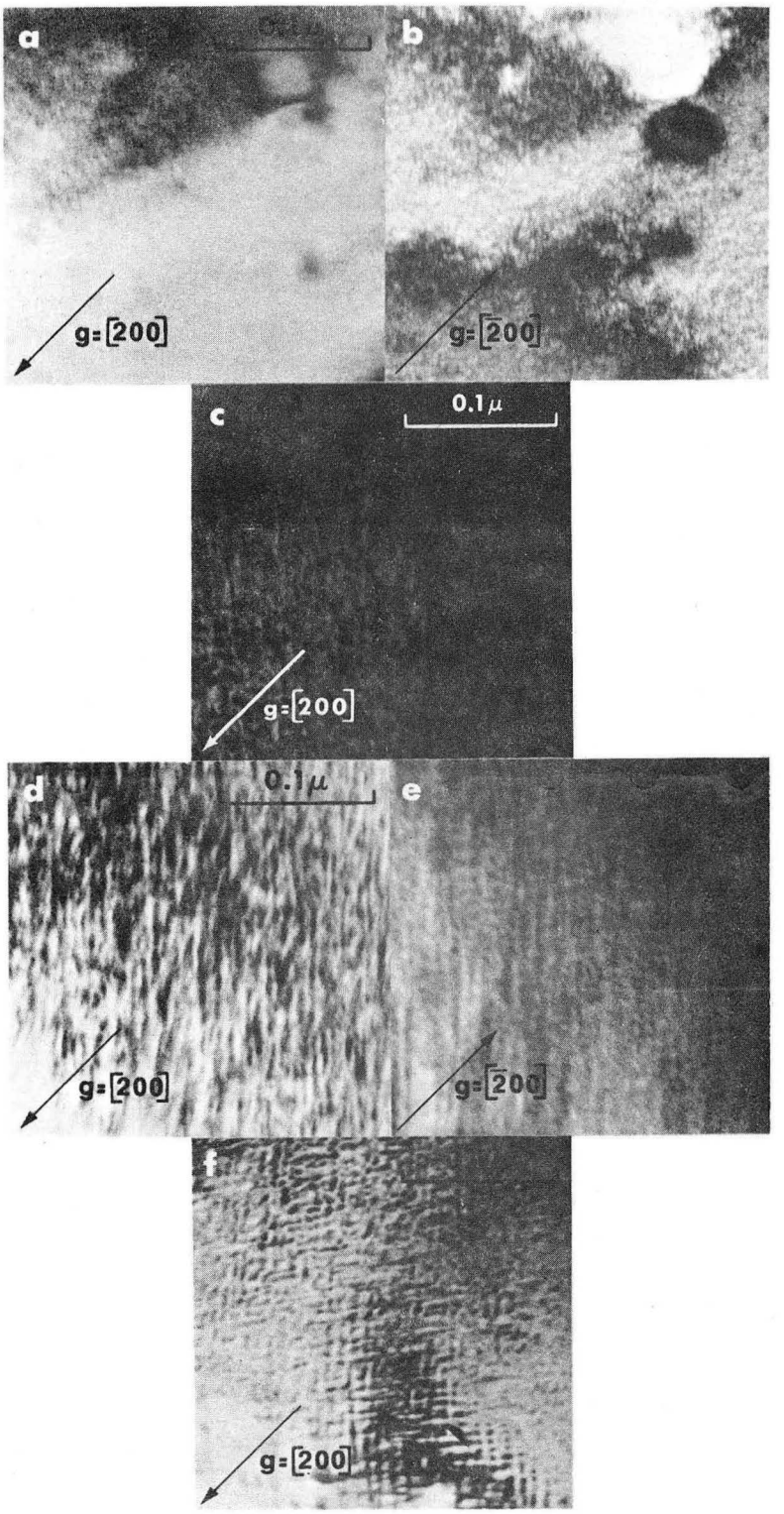

XBB 729-4718

Fig. 11

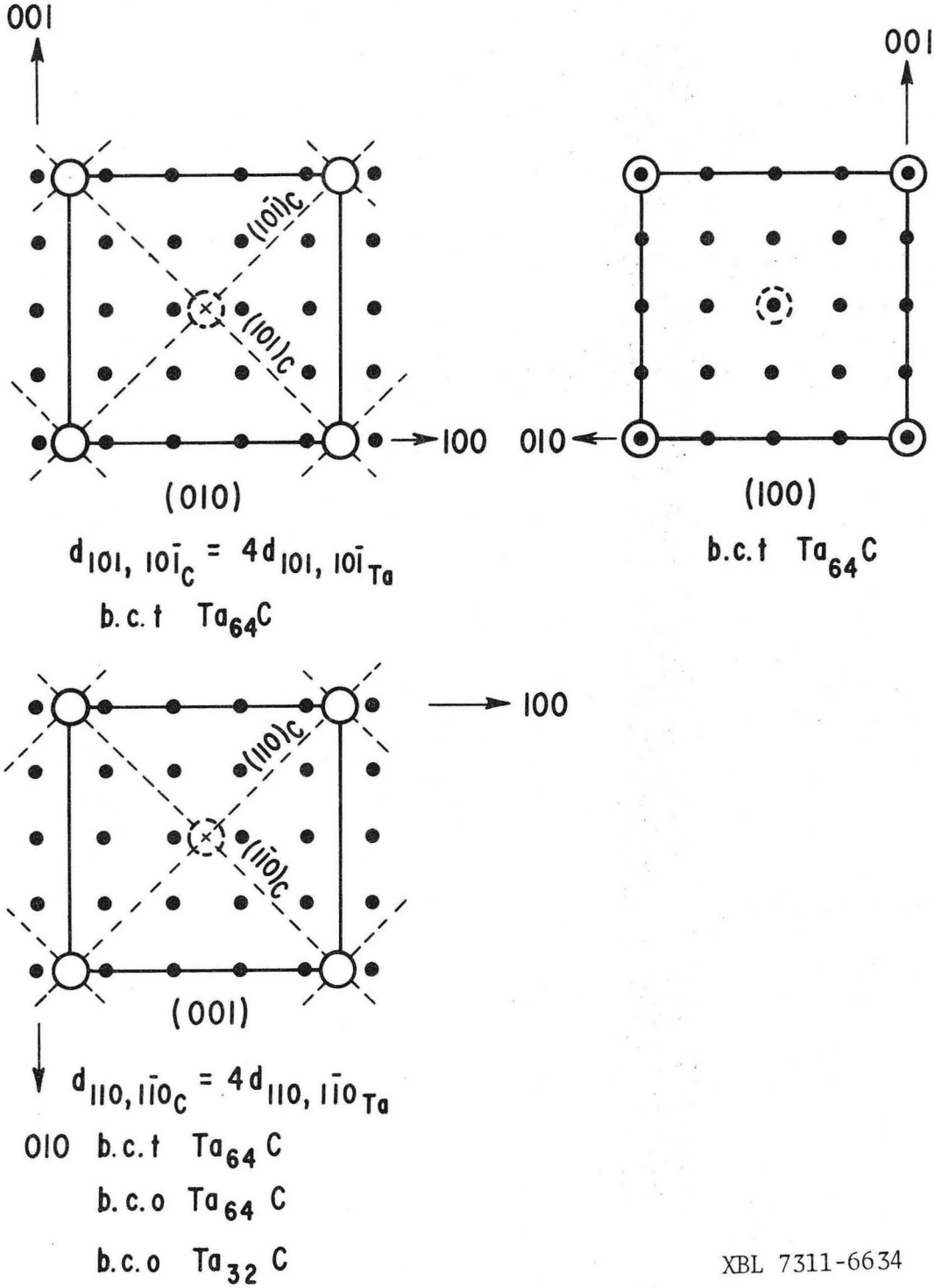

XBL 7311-6634

Fig. 12

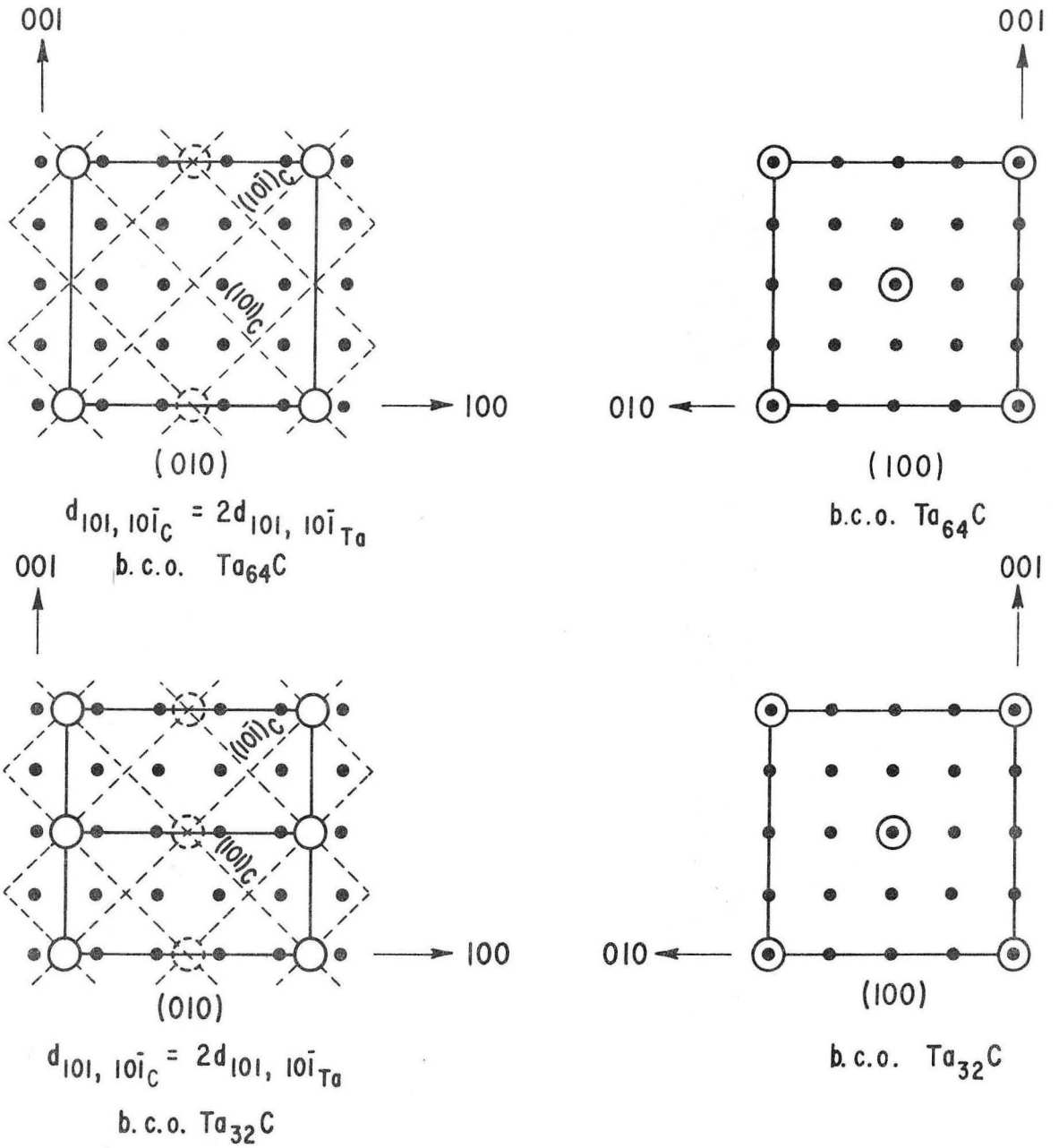

XBL 7311-6633

Fig. 12 continued

LEGAL NOTICE

This report was prepared as an account of work sponsored by the United States Government. Neither the United States nor the United States Atomic Energy Commission, nor any of their employees, nor any of their contractors, subcontractors, or their employees, makes any warranty, express or implied, or assumes any legal liability or responsibility for the accuracy, completeness or usefulness of any information, apparatus, product or process disclosed, or represents that its use would not infringe privately owned rights.

TECHNICAL INFORMATION DIVISION
LAWRENCE BERKELEY LABORATORY
UNIVERSITY OF CALIFORNIA
BERKELEY, CALIFORNIA 94720